Walter+Eliza Hall
Institute of Medical Research

Research Publication Repository

http://publications.wehi.edu.au/search/SearchPublications

This is the author's peer reviewed manuscript version of a work accepted for publication.

Publication details:	Cretney E, Leung PS, Trezise S, Newman DM, Rankin LC, Teh CE, Putoczki TL, Gray DH, Belz GT, Mielke LA, Dias S, Nutt SL. Characterization of Blimp-1 function in effector regulatory T cells. *Journal of Autoimmunity.* 2018 91:73-82
Published version is available at:	https://doi.org/ 10.1016/j.jaut.2018.04.003

Changes introduced as a result of publishing processes such as copy-editing and formatting may not be reflected in this manuscript.

©2018. This manuscript version is made available under the CC-BY-NC-ND 4.0 license
http://creativecommons.org/licenses/by-nc-nd/4.0/

Characterization of Blimp-1 function in effector regulatory T cells

Erika Cretney[1,2], Patrick SK Leung[1,2], Stephanie Trezise[1,2], Dane M Newman[1,2], Lucille C Rankin[1,2], Charis E Teh[1,2], Tracy L Putoczki[1,2], Daniel H D Gray[1,2], Gabrielle T Belz[1,2], Lisa A Mielke[1,2], Sheila Dias[1,2], Stephen L Nutt[1,2].

[1]The Walter and Eliza Hall Institute of Medical Research, Parkville, Victoria, Australia.
[2]Department of Medical Biology, The University of Melbourne, Parkville, Victoria, Australia.

Correspondence should be addressed to:
Stephen L Nutt.
The Walter and Eliza Hall Institute of Medical Research, 1G Royal Parade, Parkville, Victoria, 3052, Australia.
Ph: +61 3 9345 2483, Fax: +61 3 9347 0852, Email: nutt@wehi.edu.au

Short running title- Blimp-1 function in regulatory T cells

Keywords- Blimp-1, effector regulatory T cells, immune infiltration, transcription, IL-10.

ABSTRACT

Regulatory T (T_{reg}) cells maintain immunological tolerance in steady-state and after immune challenge. Activated T_{reg} cells can undergo further differentiation into an effector state that highly express genes critical for T_{reg} cell function, including ICOS, TIGIT and IL-10, although how this process is controlled is poorly understood. Effector T_{reg} cells also specifically express the transcriptional regulator Blimp-1 whose expression overlaps with many of the canonical markers associated with effector T_{reg} cells, although not all $ICOS^{+}TIGIT^{+}$ T_{reg} cells express Blimp-1 or IL-10. In this study, we addressed the role of Blimp-1 in effector T_{reg} cell function. Mice lacking Blimp-1 specifically in T_{reg} cells mature normally, but succumb to a multi-organ inflammatory disease later in life. Blimp-1 is not required for T_{reg} cell differentiation, with mutant mice having increased numbers of effector T_{reg} cells, but regulated a suite of genes involved in cell signaling, communication and survival, as well as being essential for the expression of the immune modulatory cytokine IL-10. Thus, Blimp-1 is a marker of effector T_{reg} cells in all contexts examined and is required for the full functionality of these cells during aging.

INTRODUCTION

Regulatory T (T_{reg}) cells play a critical role in preserving immune tolerance and homeostasis. T_{reg} cells also influence the ability of tumor cells or certain pathogens to escape immune surveillance by dampening the immune response [1-3]. The transcription factor FoxP3 is required for the generation and function of $CD4^+$ T_{reg} cells in mice and humans [4], with loss-of-function mutations in *FOXP3* triggering fatal systemic autoimmunity in both species. T_{reg} cells can be generated via two distinct pathways. The majority of T_{reg} cells are generated in the thymus, however FoxP3 expression and T_{reg} cell functionality may also be induced in peripheral $CD4^+$ T cells [3]. Thymic and peripheral T_{reg} cells are thought to play complementary and non-redundant roles in the regulation of the immune system [5, 6].

Naïve T_{reg} cells exit the thymus and migrate to a variety of lymphoid tissues, where they are able to undergo further differentiation in response to antigen [7, 8] into a cell type we term effector T_{reg} cells [9]. This differentiation process is heavily influenced by the presence of environmental cues, notably cytokines, and results in the acquisition of distinct phenotypes and effector molecules. For example, seminal studies showed that T-bet is required for T_{reg} cells to differentiate in response to T-helper 1 (Th1) stimuli [10], while STAT3 regulated T_{reg} cell responses to Th17 stimuli [11]. IRF4 was initially reported to be required for Th2 type T_{reg} cells [12]; however, subsequent studies have suggested that IRF4 is required for effector T_{reg} cells in all circumstances [13, 14]. Recently, Myb was identified as being essential for the differentiation of thymus-derived, but not peripherally-induced effector T_{reg} cells [15]. Effector T_{reg} cells express molecules directly involved in their suppressive capacity, including the inducible co-stimulator ICOS, the inhibitory receptor CTLA4, Galectin-1, the anti-inflammatory cytokine IL-10 [9], as well as the transcription factor, Blimp-1 [13].

Blimp-1, encoded by the *Prdm1* gene, is a multifunctional transcriptional regulator that has well established roles in plasma cell development and function [16, 17]. In T cells, Blimp-1 expression is induced in activated $CD4^+$ and $CD8^+$ T cells where it regulates many aspects of effector and memory differentiation [18-28]. Blimp-1 is also expressed in natural killer cells [29, 30] and dendritic cells [31], although its function in these cell types remains unclear. Interestingly, *BLIMP1/PRDM1* is a risk allele in systemic lupus erythematosus (SLE) [32] and inflammatory bowel diseases [33].

The loss of Blimp-1 in all T cells results in a lethal autoimmune pathology, that is suggestive of defective T_{reg} cell function, although isolated assays on T_{reg} cells *in vitro* and *in vivo* have shown that Blimp-1-deficient T_{reg} cells are functional [22, 34, 35]. Within T_{reg} cells Blimp-1 expression is restricted to effector T_{reg} cells where it is required for *Il10* expression [13], which itself is required for immune homeostasis at mucosal surfaces [36]. The functional consequences of Blimp-1 loss in T_{reg} cells remain uncertain, as the aforementioned studies on Blimp-1 function in T cells have all utilized pan-T cell loss of Blimp-1 or mixed bone marrow chimeras between Blimp-1-deficient and -sufficient cells. Here we have addressed the function of Blimp-1 specifically in T_{reg} cells and found that the expression of Blimp-1 defined most effector T_{reg} cells in mouse models and was essential for the full control of immune homeostasis in the mouse.

RESULTS

Blimp-1 is expressed in mouse effector T_{reg} cells and T_{FR} cells.

To examine Blimp-1 expression in mouse T_{reg} cells we made use of *Foxp3*^{RFP}*Prdm1*$^{GFP/+}$ dual reporter mice that allow us to monitor Foxp3 and Blimp-1 expression at the single cell level via expression of red fluorescent protein (RFP) and green fluorescent protein (GFP) respectively [14]. Flow cytometric analysis of splenocytes from naïve 8-week-old mice showed that 25.1±2.8% of CD4$^+$Foxp3$^+$ T_{reg} cells expressed Blimp-1/GFP (**Fig 1a**). The percentage of Blimp-1/GFP$^+$ T_{reg} cells varied depending on the age of the mouse and the T_{reg} location, with the highest percentage of Blimp-1/GFP expressing T_{reg} cells located in the colon and small intestine (**Fig 1b**).

We previously reported that Blimp-1/GFP expressing CD4$^+$CD25$^+$ cells isolated from naïve *Prdm1*$^{GFP/+}$ mice have an effector phenotype [13]. Whilst the majority of CD4$^+$CD25$^+$ cells in naïve mice are expected to express Foxp3, we next wanted to confirm whether all Blimp-1/GFP-expressing CD4$^+$Foxp3$^+$ T_{reg} cells similarly expressed activation markers. Flow cytometric analysis of spleen Blimp-1/GFP$^+$ CD4$^+$Foxp3$^+$ T_{reg} cells showed high expression of TIGIT, ICOS, CD103, KLRG1, CD44 and GITR and low expression of CD62L, consistent with an effector phenotype (**Fig 1c**).

Using quantitative RT-PCR and immunohistochemistry, T follicular regulatory (T_{FR}) cells have been shown to express Blimp-1 [37]. To examine the phenotype of Blimp-1 expressing T_{FR} cells more closely, we infected *Foxp3*^{RFP}*Prdm1*$^{GFP/+}$ mice with influenza virus (HKx31). Nine days post-infection we observed that 18.9±0.87% of CD4$^+$CXCR5^{hi}PD-1^{hi} 'T_{FH}' cells in the mediastinal (med)LN and 21.9±1.2% of 'T_{FH}' cells in the spleen expressed Foxp3 (**Fig 1d** and **Supp Fig 1a**). 22.4±2.1% of these T_{FR} cells in the medLN and 29.5±2.5% in the spleen were Blimp-1/GFP$^+$ (**Fig 1e** and **Supp Fig 1b**). Blimp-1/GFP expressing T_{FR} cells in the medLN and spleen highly expressed TIGIT and ICOS, consistent with an effector T_{reg} phenotype, and the majority expressed Neuropilin-1 (Nrp-1), a marker that has been used to identify thymus-derived T_{reg} cells (**Fig 1e** and **Supp Fig 1b)**. Together these data confirmed that Blimp-1 is expressed in a subset of T_{reg} cells in all organs examined and that the size of the Blimp-1/GFP expressing compartment varies greatly between tissues.

Cell surface markers that identify Blimp-1-expressing T_{reg} cells.

Given that Blimp-1-expressing T_{reg} cells in the spleen have an effector phenotype (**Fig 1c**), we were interested whether Blimp-1-expressing T_{reg} cells at other sites might possess a similar phenotype. Nrp-1 was expressed in the majority of Blimp-1-expressing T_{reg} cells in thymus, blood, liver, lung, peripheral (p)LN and spleen, suggesting that they were predominantly thymus-derived T_{reg} cells (**Fig 2a)**. The majority of Blimp-1-expressing T_{reg} cells in the mesenteric (m)LN, Peyer's patches (PP), colon lamina propria lymphocytes (LPL), small intestine (si) intraepithelial lymphocytes (IEL) and siLPL were Nrp-1$^-$, suggesting that these cells were generated in the periphery (**Fig 2a, b)**. The majority of Blimp-1-expressing T_{reg} cells highly expressed the inducible T-cell costimulator ICOS, though a lower percentage of ICOS expression was found on Blimp-1-expressing T_{reg} cells in the gut (**Fig 2a)**. The inhibitory molecule TIGIT was expressed on more than 50% of Blimp-1-expressing T_{reg} cells in the thymus, blood, lung, mLN, pLN and spleen, in sharp contrast to liver and gut Blimp-1-expressing T_{reg} cells, most of which were TIGIT$^-$ **(Fig 2a, b)**.

Although the reporter function of the *Prdm1*^{GFP} allele can be used to identify the Blimp-1-expressing T_{reg} cells, we wanted to develop an alternate non-transgenic gating strategy to identify this cell population. Using cells isolated from *Foxp3*^{RFP}*Prdm1*$^{GFP/+}$ mice we determined that an ICOS$^+$TIGIT$^+$ gate (R1 in **Fig 2c**) within the CD4$^+$Foxp3$^+$ T_{reg} population

encompassed the vast majority of splenic Blimp-1-GFP$^+$ T_{reg} cells; however, the overlap of the populations was not absolute, as only half of the ICOS$^+$TIGIT$^+$ T_{reg} cells within this gate expressed Blimp-1/GFP (R2 in **Fig 2c**). This trend was also observed in CD4$^+$Foxp3$^+$ T_{reg} cells examined in pLN, mLN, liver, lung, blood and PP **(Fig 2d)**. These data indicate that that while all Blimp-1/GFP$^+$ T_{reg} cells fall into the ICOS$^+$TIGIT$^+$ gate, ICOS and TIGIT expression appears to precede Blimp-1 as many ICOS$^+$TIGIT$^+$ cells have not yet activated Blimp-1/GFP expression. Nevertheless, the use of ICOS and TIGIT was a reasonable approximation of the effector T_{reg} cell compartment in absence of the *Prdm1*^{GFP} reporter allele.

Increased activation of T_{reg} cells without Blimp-1.

To examine the function of Blimp-1 in the T_{reg} compartment we generated *Prdm1*$^{fl/fl}$*Foxp3*$^{YFP\text{-}Cre}$ mice. PCR analysis showed highly efficient inactivation of *Prdm1* in purified CD4$^+$Foxp3$^+$ cells isolated from *Prdm1*$^{fl/fl}$*Foxp3*$^{YFP\text{-}Cre}$ mice, but not in genomic DNA extracted from the tail of control C57Bl/6 or *Prdm1*$^{fl/fl}$ mice **(Fig 3a)**. In keeping with a previous report of leaky expression of the *Foxp3*$^{YFP\text{-}Cre}$ allele in non-T_{reg} cells [38], we observed some Cre activity in purified CD4$^+$Foxp3$^-$, CD8$^+$ and B220$^+$ cells isolated from *Prdm1*$^{fl/fl}$*Foxp3*$^{YFP\text{-}Cre}$ mice **(Fig 3a)**. Although the degree of leakiness of the *Foxp3*$^{YFP\text{-}Cre}$ allele differed between individual mice, we observed evidence of deletion in non-T_{reg} cells in every individual mouse tested.

Prdm1$^{fl/fl}$*Foxp3*$^{YFP\text{-}Cre}$ mice developed normally and young adults showed no pathological phenotype, suggesting that T_{reg} cell function was grossly intact without Blimp-1. Examination of the splenic T_{reg} cell compartment in 8 week old *Prdm1*$^{fl/fl}$*Foxp3*$^{YFP\text{-}Cre}$ mice revealed a greater proportion of Foxp3$^+$ T_{reg} cells (as a proportion of CD4$^+$ cells) compared to control mice **(Fig 3b)**. A greater proportion of *Blimp1*$^{fl/fl}$*Foxp3*$^{YFP\text{-}Cre}$ splenic T_{reg} cells expressed ICOS and CD103, with a lower expression of CD62L, consistent with an activated phenotype **(Fig 3b)**. The expanded proportion of Foxp3$^+$ T_{reg} cells and ICOS expression was also observed in most lymphoid and non-lymphoid tissues **(Fig 3c)**. Thus, loss of Blimp-1 resulted in perturbed homeostasis of the T_{reg} cell lineage.

Immunopathology in aged mice lacking Blimp-1 in T_{reg} cells

To further examine the effect of Blimp-1-deficiency in T_{reg} cells, we aged *Prdm1*$^{fl/fl}$*Foxp3*$^{YFP\text{-}Cre}$ mice for up to 700 days. *Prdm1*$^{fl/fl}$*Foxp3*$^{YFP\text{-}Cre}$ mice started to present with clinical illness, including weight loss, lethargy and disheveled appearance at around day 110 and all mice had to be culled for ethical reasons by day 650. As expected, the majority of control mice remained healthy during this time period **(Fig 4a)**. Given the role of T_{reg} cells in restraining autoimmunity and inflammation, and the genetic association of *PRDM1* with SLE [32], we examined serum of aged mice for the presence of antinuclear antibodies (ANA), a characteristic feature of the disease. At 1 year of age, modestly higher amounts of ANA were observed in *Prdm1*$^{fl/fl}$*Foxp3*$^{YFP\text{-}Cre}$ sera compared to controls. Increased serum titers of ANA was also observed in aged *Prdm1*$^{fl/fl}$*Foxp3*$^{YFP\text{-}Cre}$ mice culled for ethical reasons **(Fig 4b)**, although it should be noted that the elevated serum ANA titers remained well below that measured from *Lyn*$^{-/-}$ mice, a well characterized model of SLE [39].

Autopsy of *Prdm1*$^{fl/fl}$*Foxp3*$^{YFP\text{-}Cre}$ mice revealed that many mice developed splenomegaly and lymphadenopathy with age **(Fig 4c** and data not shown**)**. Abnormalities were also observed in organs including the liver, lung and gastrointestinal tract **(Fig 4c** and data not shown**)**. Histological analysis of multiple organs revealed variable signatures of autoimmune pathology in salivary gland, pancreas and gastrointestinal tract, although the exact organ targeted varied widely between individual mice **(Fig 4d)**. Adoptive transfer of splenocytes from aged *Prdm1*$^{fl/fl}$*Foxp3*$^{YFP\text{-}Cre}$ mice could transfer pathology to *Rag1*$^{-/-}$ recipients suggesting an autoimmune component. An example of this data is shown in **Fig 4c** where splenocytes from mouse #168 (showing multi-organ pathology) were transferred into a *Rag1*$^{-/-}$ recipient. The recipient (P1 Rag #168) was culled due to weight loss after 13.6 weeks and showed a similar multi-organ pathology to the founder **(Fig 4c)**.

Similar to 8 week old *Prdm1*$^{fl/fl}$*Foxp3*$^{YFP\text{-}Cre}$ mice **(Fig 3c)**, aged *Prdm1*$^{fl/fl}$*Foxp3*$^{YFP\text{-}Cre}$ mice also contained activated T_{reg} cells, expressing high levels of ICOS and TIGIT in a number of locations throughout the body **(Fig 4e)**. In keeping with a failure in immune tolerance, increased ICOS and TIGIT expression was also observed in conventional $CD4^+Foxp3^-$ and $CD8^+$ cells isolated from aged *Prdm1*$^{fl/fl}$*Foxp3*$^{YFP\text{-}Cre}$ mice, evidence of abnormally high conventional T cell activation **(Supp Fig 2)**. In summary, Blimp-1 function in T_{reg} cells was essential to maintain immune homeostasis throughout life.

Identification of Blimp-1 regulated genes in T_{reg} cells.

To systematically identify Blimp-1 regulated genes in T_{reg} cells we have analyzed microarray data from Blimp-1 sufficient (*Prdm1*$^{GFP/+}$) and Blimp-1 deficient (*Prdm1*$^{GFP/GFP}$) T_{reg} cells. Importantly, in both samples T_{reg} cells were sorted as GFP$^+$ and thus transcribing the *Prdm1*-null allele [13]. Global analysis revealed 744 differentially expressed genes in the absence of Blimp-1. 468 genes whose expression increased without Blimp-1 and 276 down regulated genes **(Figure 5a).** We have previously identified a signature of 1769 genes that are differentially expressed in effector T_{reg} cells compared to naive or activated phenotype T_{reg} cells [15]. Notably, Blimp-1 loss impacted on the expression of only 7.8% (138 genes) of the effector T_{reg} cell signature genes, suggesting that effector T_{reg} cells identity is maintained normally in the absence of Blimp-1 **(Figure 5b).** Instead, pathway analysis and manual inspection revealed roles for Blimp-1 in controlling signal transduction at various points, cell communication, adhesion and death **(Figure 5c,d)**. In keeping with these conclusions, the expression of multiple members of the chemokine and chemokine receptor family was dysregulated without Blimp-1. Blimp-1 loss also impacted on the expression of multiple other transcription factors including *Rorc* (RORγt), *Tbx21* (T-bet), *Tcf7*, *Cebpa, Vdr* (Vitamin D receptor), *Id3* and *Irf8*, thus linking its activity with multiple components of the gene regulatory network of effector T_{reg} cells **(Figure 5c)**. Finally aspects of functionality were impacted by the loss of Blimp-1, including reduced expression of *Fasl, Havcr2* (Tim-3) and *Klrg1* and the genes encoding the IL-12 and IL-18 receptors.

The gene encoding IL-10 was the third most downregulated gene in our dataset (**Figure 5c**). We previously used mixed bone marrow chimeric mice to demonstrate that *Il10* is a direct target gene of Blimp-1 [13]. To confirm this finding, we used quantitative RT-PCR to examine *Il10* expression in T_{reg} cells isolated from *Prdm1*$^{fl/fl}$*Foxp3*$^{YFP\text{-}Cre}$ mice. High *Il10* expression was observed in purified IL-10$^+$ T_{reg} cells isolated from *Foxp3*^{RFP}*Il10*^{GFP} mice and in Blimp-1/GFP$^+$ T_{reg} cells **(Fig 5e)**. In contrast, *Il10* expression was at background levels in T_{reg} cells from *Prdm1*$^{fl/fl}$*Foxp3*$^{YFP\text{-}Cre}$ mice **(Fig 5e)**, thus confirming that *Il10* expression in T_{reg} cells required Blimp-1. Taken together these data demonstrate that Blimp-1 is not required for effector T_{reg} cell formation, survival or identity, but instead Blimp-1 plays a

pleiotropic role in T_{reg} cells influencing multiple biological processes, that ultimately are required for life long immunological tolerance.

DISCUSSION

T_{reg} cells are essential for immune tolerance and homeostasis, as their absence results in catastrophic inflammatory disease and early lethality. Although most aspects of T_{reg} cell biology rely on the continued expression and function of FoxP3, it has also become apparent that phenotypically mature or "naïve" T_{reg} cells undergo a multi-step differentiation process, generating first an "activated" state, followed by an effector T_{reg} cell stage [9]. We have previously proposed that the expression of Blimp-1 defines this effector T_{reg} cell stage, and that Blimp1 expression is in turn induced by IRF4 that is essential for the development of all effector T_{reg} cells [13]. Here we have further characterized the Blimp-1/GFP$^+$ effector T_{reg} cell compartment and determined the impact of inactivating Blimp-1 only in T_{reg} cells.

Similar to the conventional CD4$^+$ T cells, the differentiation and diversification of activated T_{reg} cells occurs in response to cytokine signals from the cellular environment [9, 40-43]. This diversification generates activated and effector T_{reg} cells with Th1, Th2, Th17 and T follicular helper cell like characteristics. Moreover, distinct tissue-resident T_{reg} cell populations occur in non-lymphoid organs, including adipose tissue [14, 44]. The evidence to date, from this study and others, suggests that the IRF4-mediated induction of Blimp-1 is a common feature of effector T_{reg} cells in all these settings [13, 14]. Blimp-1 may however impact of subsequent T_{reg} cell diversification as the expression of many transcription factors known to be important in T_{reg} cell subsets including *Rorc* [45], *Tbx21* [10, 46], *Tcf7* [47, 48], *Id3* [49, 50], *Irf8* [51] and the cell surface marker *Klrg1* [52] were dysregulated in the absence of Blimp-1.

T_{reg} cells are known to be either thymus-derived, representing a large proportion of T_{reg} cells in steady-state lymphoid organs, or peripherally induced from conventional CD4$^+$ T cells, predominating in mucosal sites such as the gastrointestinal tract [3]. We have recently reported that the transcriptional control of effector T_{reg} cell differentiation derived from these two pathways is distinct, as the loss of the transcription factor Myb in T_{reg} cells blocks effector differentiation of thymus-derived, but not peripherally induced, T_{reg} cells [15]. Our

current analysis shows that, in contrast to Myb, Blimp-1 is expressed in effector T_{reg} cells from both pathways suggesting that it is an important component in a conserved effector T_{reg} cell program that is the end-point of all T_{reg} cell differentiation pathways.

Although Blimp-1/GFP expression discriminates effector T_{reg} cells, the development of a non-transgenic approach to identify these cells with surrogate markers is clearly desirable. Comparison of Blimp-1/GFP expression with all other known markers of the differentiation process, including ICOS, TIGIT, CD103, KLRG1, suggested an imperfect relationship, with approximately half of the $FoxP3^+ICOS^+TIGIT^+$ cells expressing Blimp-1. One model to explain this observation is that within the activated ($CD62L^-CD44^+$) T_{reg} cell gate are two stages of differentiation, the $Blimp\text{-}1^-/GFP^-ICOS^+TIGIT^+$ cells and the fully mature $Blimp\text{-}1^+/GFP^+ICOS^+TIGIT^+$ effector T_{reg} cells. Genome wide transcriptomic approaches are needed to explore this hypothesis more thoroughly. The situation is reversed for CD103 and KLRG1, where approximately 50% of $Blimp\text{-}1/GFP^+ICOS^+TIGIT^+$ effector T_{reg} cells express either marker, potentially reflecting the diversity of the effector pool.

Mice lacking Blimp-1 in either all blood cells or specifically in T cells have a propensity to develop autoimmune pathology, characterized by severe inflammation of mucosal surfaces [22, 34, 35]. While these studies may suggest a role for Blimp-1 in T_{reg} cells, the many other functions of Blimp-1 in differentiation of $CD4^+$ and $CD8^+$ T cells and the regulation of IL-10 expression in multiple cell types, including Tr1 and Th1 cells, were also potentially involved in the phenotype observed [19-21, 23, 25-27]. Moreover, early studies showed that Blimp-1-deficient T_{reg} cells were able to appropriately regulate conventional $CD4^+$ T cells in *in vitro* and *in vivo* assays [19, 22], arguing against a profound loss of T_{reg} cell function without Blimp-1. In this study, we directly tested the importance of Blimp-1 specifically in T_{reg} cells via conditional deletion in $Foxp3^+$ cells. We found increased production of T_{reg} cells that displayed a highly activated state. Nevertheless, mice lacking Blimp-1 in T_{reg} cells were healthy until approximately day 120, a finding that agrees well with a recent study that found only mild intestinal inflammation in younger mice lacking Blimp-1 in T_{reg} cells [18]. However upon more prolonged aging, all $Prdm1^{fl/fl}Foxp3^{YFP\text{-}Cre}$ mice developed clinical signs of an inflammatory/autoimmune disease with a half-life of approximately 400 days. The moribund mice showed broad inflammatory features, including splenomegaly and lymphadenopathy, immune infiltration into liver, lung, salivary glands and pancreas that

suggest stochastic or environmental triggers that target particular organs. This disease progression is markedly slower than that observed in mice lacking T_{reg} cells entirely which show severe symptoms by week 3 [53]. Thus, Blimp-1 plays a role in maintaining T_{reg} cell function specifically during the aging process. One notable target gene of Blimp-1 is *Il10*, whose expression was absent in Blimp-1-deficient T_{reg} cells. T_{reg} cell derived IL-10 is known to be important for immune tolerance at mucosal sites [36], and it is likely that loss of IL-10 is one of the major contributors to the pathology observed.

In summary, this study shows that Blimp-1 is expressed in mouse effector T_{reg} cells regardless of their origin. Blimp-1 plays an important role in maintaining effector T_{reg} cell function and immune homeostasis in aged mice. As *PRDM1* is a risk allele in several autoimmune diseases including SLE and inflammatory bowel diseases [32, 33], it will be important in the future to assess if BLIMP-1 expression and effector T_{reg} cell function in general, is altered in individuals with these conditions.

ACKNOWLEDGEMENTS

We thank Jamie Leahy and Liana Mackiewicz for technical support and the WEHI Flow Cytometry Laboratory staff for assistance in cell sorting. We thank Alexander Rudensky for mice. Research was supported by the National Health and Medical Research Council of Australia (program grant #1054925 to SLN, project grant #1047313 to EC, project grant #1078763 to DHDG and fellowships to EC, SLN, CET, DHDG and GTB). This work was made possible through Victorian State Government Operational Infrastructure Support and Australian Government NHMRC IRIIS.

There are no competing financial interests in relation to the work described.

MATERIAL AND METHODS

Mice

Prdm1$^{+/GFP}$ [54] and *Prdm1*$^{fl/fl}$ [19] mice were previously described. C57BL/6 wild-type, C57BL/6-Ly5.1 and *Rag1*$^{-/-}$ mice were from the Walter and Eliza Hall Institute of Medical Research (WEHI) breeding facility. *Foxp3*^{RFP} [55] and *Il10*^{GFP} [56] mice were from Jackson

Laboratory. *Foxp3*$^{YFP\text{-}Cre}$ [36] mice were provided by Alexander Rudensky (MSKCC, New York, USA). All mice were bred and maintained on a C57BL/6 background at the WEHI. Animal experiments were done according to Animal Experimental Ethics Committee guidelines and approval.

Flow cytometry

Cells were surface stained with various fluorochrome-labelled mAbs **(Supp Table 1)** in the presence of 2.4G2 to block Fc-receptors. SYTOX^{TM} Blue dead cell stain (Life Technologies) was added immediately before flow cytometry analysis. For intracellular staining, cells were first stained with Fixable Viability Dye eFluor® 506 (eBioscience) according to manufacturer's instruction. After surface staining, cells were fixed with eBioscience Transcription Factor Staining Buffer Set (eBioscience). Fixed cells were then stained with fluorescently conjugated Foxp3 mAbs as indicated. Labeled cells were examined on a BD FACSCanto II or LSR Fortessa x20 (BD Biosciences) flow cytometer and analysis was carried out using Flowjo software.

Influenza Infection

Mice were inoculated intranasally with $1x10^4$ plaque-forming units of HKx31 (H3N2) influenza virus. Analysis of the lung-draining mediastinal lymph node and the spleen was performed at 9 days after infection at the peak of the anti-viral response.

Genotyping for *Prdm1* inactivation

Single cell suspensions were made from the spleens of *Prdm1*$^{fl/fl}$*Foxp3*$^{YFP\text{-}Cre}$ and control mice as described above, stained with CD4, CD8, and B220 mAb, and sorted into $CD4^+Foxp3^-$, $CD4^+Foxp3^+$, $CD8^+$ and $B220^+$ cells on a BD Influx (BD Bioscience) flow cytometer. Cells were then lysed and made into crude DNA using DirectPCR Lysis Reagent (Viagen) according to the manufacturer's protocol. The DNA was then used in a PCR reaction with GoTaq Green Master Mix (Promega) to determine the presence of wild type (611bp), floxed (765bp), or deleted (646bp) *Prdm1* alleles as described previously [19].

Quantitation of *Il10* expression

Total RNA from sorted splenocytes was extracted using a RNeasy Plus Mini Kit (Qiagen), and RNA concentration was determined using the Qubit 2.0 Fluorometer (Invitrogen) according to manufacturer's instructions. RNA was reverse-transcribed into cDNA using iScript Reverse Transcription Supermix for RT-qPCR (Bio-Rad) following the manufacturers' protocols. Real-time PCR for *Il10* (Sense: 5'-GAAGACCCTCAGGATGCGG -3' and antisense 5'- CCTGCTCCACTGCCTTGCT-3') was performed with SensiFAST SYBR No-ROX kit (BIOLINE) according to the manufacturer's instructions. Results were expressed as normalized expression calculated from mean reading of sample triplicates, with *Hprt1* as the reference gene (Sense: 5'-GGGGGCTATAAGTTCTTTGC-3' and antisense 5'-TCCAACACTTCGAGAGGTCC-3').

Anti-nuclear antibody ELISA

RELISA ANA Screening Test System (Immuno Concepts) was used to detect antinuclear antibodies (ANA) present in the mouse serum according to manufacturer's protocol, except that goat anti-mouse IgG1, IgG2a and IgG2b conjugated to horseradish peroxidase (HRP) (Southern Biotech) were used as the secondary antibody instead of the human specific RELISA Enzyme Antibody Reagent provided. Results were analyzed and expressed relative to the serum ANA level from a 48 week *Lyn*$^{-/-}$ mouse (provided by David Tarlinton, Monash University, Melbourne, Australia).

Histopathological scoring of salivary glands, pancreas, colon and small intestine

Following ethical euthanasia of mouse, the entire gut was removed. Colon was separated from the end of cecum and opened longitudinally and rinsed gently with PBS to remove the bowel content. Colon is then rolled from the distal end towards the proximal end. Small intestine was separated from the end of the stomach to the start of the cecum. 3-4 1cm sections were cut from the proximal, middle and distal part. Colon and small pieces sections and whole salivary glands and pancreas were fixed in neutral-buffed formalin for a minimal

of 24 hours before embedding in paraffin and sectioning. Slides were stained in Hemotoxylin and Eosin. Histopathological scoring of the gastrointestinal tract was performed in a blinded manner as described previously [57], on a scale of 0 (normal) to 5 (severe). *Pancreas*: (0) No pancreatitis; (1) Perivascular/periductal lymphocyte infiltration; (2) Small patches of lymphocyte infiltration in the exocrine tissue; (3) Extensive infiltration in the exocrine pancreatic tissue and destruction of <50% of the exocrine acinar tissue; (4) Extensive infiltration in the exocrine pancreatic tissue and destruction of 50–90% of the exocrine acinar tissue; (5) Extensive infiltration in the exocrine pancreatic tissue and complete absence of exocrine acinar tissue. *Submandibular salivary gland*: (0) No sialoadenitis; (1) Multiple small patches of perivascular/periductal lymphocyte infiltration; (2) Small patches of lymphocyte infiltration in the supporting tissue, almost complete absence of serous acini, and no destruction of mucous acini; (3) Diffuse lymphocytic infiltration, complete absence of serous acini, and destruction of less than 50% of the mucous acinar tissue; (4) Diffuse lymphocytic infiltration, complete absence of serous acini and destruction of 50– 90% of the mucous acinar tissue; (5) Diffuse lymphocytic infiltration, complete absence of serous acini, and >90% absence of mucous acinar tissue.

Bioinformatics

The microarray data comparing the Blimp-1/GFP^{+} T_{reg} cells from *Prdm1*$^{GFP/+}$ and *Prdm1*$^{GFP/GFP}$ mice has been partially described previously [13] and is publicly available at the Gene Expression Omnibus (www.ncbi.nlm.nih.gov/geo) under the accession GSE27143. The effector T_{reg} cell RNAseq data (GSE72494) is from [15]. Gene ontology analyses were obtained from PANTHER Classification System version 11.0 [58]. Statistical overrepresentation test was performed on activated and repressed genes using PANTHER GO-Slim Biological Process. Only results with p value<0.05, and positive fold enrichment >1 are displayed.

Statistical Analysis

Statistical analyses were carried out using Graph Pad Prism software. Significant difference in mean fluorescence intensity (MFI) or percentage of cells were determined by unpaired t

tests, assuming a Gaussian distribution with Welch's correction. Values of $P < 0.05$ were considered significant. A one-sample t test was used for normalized data.

REFERENCES

[1] D. Burzyn, C. Benoist, D. Mathis. Regulatory T cells in nonlymphoid tissues. Nat Immunol, 2013;14:1007-13.

[2] S. Z. Josefowicz, L. F. Lu, A. Y. Rudensky. Regulatory T cells: mechanisms of differentiation and function. Annual review of immunology, 2012;30:531-64.

[3] T. Yamaguchi, J. B. Wing, S. Sakaguchi. Two modes of immune suppression by Foxp3(+) regulatory T cells under inflammatory or non-inflammatory conditions. Seminars in Immunology, 2011;23:424-30.

[4] A. Y. Rudensky. Regulatory T cells and Foxp3. Immunol Rev, 2011;241:260-8.

[5] D. Haribhai, J. B. Williams, S. Jia, D. Nickerson, E. G. Schmitt, B. Edwards *et al.* A requisite role for induced regulatory T cells in tolerance based on expanding antigen receptor diversity. Immunity, 2011;35:109-22.

[6] S. Z. Josefowicz, R. E. Niec, H. Y. Kim, P. Treuting, T. Chinen, Y. Zheng *et al.* Extrathymically generated regulatory T cells control mucosal TH2 inflammation. Nature, 2012;482:395-9.

[7] A. G. Levine, A. Arvey, W. Jin, A. Y. Rudensky. Continuous requirement for the TCR in regulatory T cell function. Nature Immunology, 2014;15:1070-8.

[8] J. C. Vahl, C. Drees, K. Heger, S. Heink, J. C. Fischer, J. Nedjic *et al.* Continuous T cell receptor signals maintain a functional regulatory T cell pool. Immunity, 2014;41:722-36.

[9] E. Cretney, A. Kallies, S. L. Nutt. Differentiation and function of Foxp3(+) effector regulatory T cells. Trends in immunology, 2013;34:74-80.

[10] M. A. Koch, G. Tucker-Heard, N. R. Perdue, J. R. Killebrew, K. B. Urdahl, D. J. Campbell. The transcription factor T-bet controls regulatory T cell homeostasis and function during type 1 inflammation. Nat Immunol, 2009;10:595-602.

[11] A. Chaudhry, D. Rudra, P. Treuting, R. M. Samstein, Y. Liang, A. Kas *et al.* CD4+ regulatory T cells control TH17 responses in a Stat3-dependent manner. Science, 2009;326:986-91.

[12] Y. Zheng, A. Chaudhry, A. Kas, P. deRoos, J. M. Kim, T. T. Chu *et al.* Regulatory T-cell suppressor program co-opts transcription factor IRF4 to control T(H)2 responses. Nature, 2009;458:351-6.

[13] E. Cretney, A. Xin, W. Shi, M. Minnich, F. Masson, M. Miasari *et al.* The transcription factors Blimp-1 and IRF4 jointly control the differentiation and function of effector regulatory T cells. Nat Immunol, 2011;12:304-11.

[14] A. Vasanthakumar, K. Moro, A. Xin, Y. Liao, R. Gloury, S. Kawamoto *et al.* The transcriptional regulators IRF4, BATF and IL-33 orchestrate development and maintenance of adipose tissue-resident regulatory T cells. Nature Immunology, 2015;16:276-85.

[15] S. Dias, A. D'Amico, E. Cretney, Y. Liao, J. Tellier, C. Bruggeman *et al.* Effector Regulatory T Cell Differentiation and Immune Homeostasis Depend on the Transcription Factor Myb. Immunity, 2017;46:78-91.
[16] M. Minnich, H. Tagoh, P. Bonelt, E. Axelsson, M. Fischer, B. Cebolla *et al.* Multifunctional role of the transcription factor Blimp-1 in coordinating plasma cell differentiation. Nat Immunol, 2016;17:331-43.
[17] J. Tellier, W. Shi, M. Minnich, Y. Liao, S. Crawford, G. K. Smyth *et al.* Blimp-1 controls plasma cell function through the regulation of immunoglobulin secretion and the unfolded protein response. Nat Immunol, 2016;17:323-30.
[18] R. Bankoti, C. Ogawa, T. Nguyen, L. Emadi, M. Couse, S. Salehi *et al.* Differential regulation of Effector and Regulatory T cell function by Blimp1. Sci Rep, 2017;7:12078.
[19] A. Kallies, A. Xin, G. T. Belz, S. L. Nutt. Blimp-1 transcription factor is required for the differentiation of effector CD8(+) T cells and memory responses. Immunity, 2009;31:283-95.
[20] P. Lu, B. A. Youngblood, J. W. Austin, A. U. Mohammed, R. Butler, R. Ahmed *et al.* Blimp-1 represses CD8 T cell expression of PD-1 using a feed-forward transcriptional circuit during acute viral infection. J Exp Med, 2014;211:515-27.
[21] L. K. Mackay, M. Minnich, N. A. Kragten, Y. Liao, B. Nota, C. Seillet *et al.* Hobit and Blimp1 instruct a universal transcriptional program of tissue residency in lymphocytes. Science, 2016;352:459-63.
[22] G. A. Martins, L. Cimmino, M. Shapiro-Shelef, M. Szabolcs, A. Herron, E. Magnusdottir *et al.* Transcriptional repressor Blimp-1 regulates T cell homeostasis and function. Nat Immunol, 2006;7:457-65.
[23] M. Montes de Oca, R. Kumar, F. de Labastida Rivera, F. H. Amante, M. Sheel, R. J. Faleiro *et al.* Blimp-1-Dependent IL-10 Production by Tr1 Cells Regulates TNF-Mediated Tissue Pathology. PLoS Pathog, 2016;12:e1005398.
[24] I. A. Parish, H. D. Marshall, M. M. Staron, P. A. Lang, A. Brustle, J. H. Chen *et al.* Chronic viral infection promotes sustained Th1-derived immunoregulatory IL-10 via BLIMP-1. J Clin Invest, 2014;124:3455-68.
[25] R. L. Rutishauser, G. A. Martins, S. Kalachikov, A. Chandele, I. A. Parish, E. Meffre *et al.* Transcriptional repressor Blimp-1 promotes CD8(+) T cell terminal differentiation and represses the acquisition of central memory T cell properties. Immunity, 2009;31:296-308.
[26] H. Shin, S. D. Blackburn, A. M. Intlekofer, C. Kao, J. M. Angelosanto, S. L. Reiner *et al.* A role for the transcriptional repressor Blimp-1 in CD8(+) T cell exhaustion during chronic viral infection. Immunity, 2009;31:309-20.
[27] H. M. Shin, V. N. Kapoor, T. Guan, S. M. Kaech, R. M. Welsh, L. J. Berg. Epigenetic modifications induced by Blimp-1 Regulate CD8(+) T cell memory progression during acute virus infection. Immunity, 2013;39:661-75.
[28] A. Xin, F. Masson, Y. Liao, S. Preston, T. Guan, R. Gloury *et al.* A molecular threshold for effector CD8(+) T cell differentiation controlled by transcription factors Blimp-1 and T-bet. Nat Immunol, 2016;17:422-32.
[29] A. Kallies, S. Carotta, N. D. Huntington, N. J. Bernard, D. M. Tarlinton, M. J. Smyth *et al.* A role for Blimp1 in the transcriptional network controlling natural killer cell maturation. Blood, 2011;117:1869-79.

[30] M. A. Smith, M. Maurin, H. I. Cho, B. Becknell, A. G. Freud, J. Yu *et al.* PRDM1/Blimp-1 controls effector cytokine production in human NK cells. J Immunol, 2010;185:6058-67.
[31] S. J. Kim, Y. R. Zou, J. Goldstein, B. Reizis, B. Diamond. Tolerogenic function of Blimp-1 in dendritic cells. J Exp Med, 2011;208:2193-9.
[32] V. Gateva, J. K. Sandling, G. Hom, K. E. Taylor, S. A. Chung, X. Sun *et al.* A large-scale replication study identifies TNIP1, PRDM1, JAZF1, UHRF1BP1 and IL10 as risk loci for systemic lupus erythematosus. Nat Genet, 2009;41:1228-33.
[33] W. T. Uniken Venema, M. D. Voskuil, G. Dijkstra, R. K. Weersma, E. A. Festen. The genetic background of inflammatory bowel disease: from correlation to causality. J Pathol, 2017;241:146-58.
[34] A. Kallies, E. D. Hawkins, G. T. Belz, D. Metcalf, M. Hommel, L. M. Corcoran *et al.* Transcriptional repressor Blimp-1 is essential for T cell homeostasis and self-tolerance. Nat Immunol, 2006;7:466-74.
[35] M. H. Lin, L. T. Yeh, S. J. Chen, H. Y. Chiou, C. C. Chu, L. B. Yen *et al.* T cell-specific BLIMP-1 deficiency exacerbates experimental autoimmune encephalomyelitis in nonobese diabetic mice by increasing Th1 and Th17 cells. Clin Immunol, 2014;151:101-13.
[36] Y. P. Rubtsov, J. P. Rasmussen, E. Y. Chi, J. Fontenot, L. Castelli, X. Ye *et al.* Regulatory T cell-derived interleukin-10 limits inflammation at environmental interfaces. Immunity, 2008;28:546-58.
[37] M. A. Linterman, W. Pierson, S. K. Lee, A. Kallies, S. Kawamoto, T. F. Rayner *et al.* Foxp3+ follicular regulatory T cells control the germinal center response. Nat Med, 2011;17:975-82.
[38] D. Franckaert, J. Dooley, E. Roos, S. Floess, J. Huehn, H. Luche *et al.* Promiscuous Foxp3-cre activity reveals a differential requirement for CD28 in Foxp3(+) and Foxp3(-) T cells. Immunol Cell Biol, 2015;93:417-23.
[39] M. L. Hibbs, D. M. Tarlinton, J. Armes, D. Grail, G. Hodgson, R. Maglitto *et al.* Multiple defects in the immune system of Lyn-deficient mice, culminating in autoimmune disease. Cell, 1995;83:301-11.
[40] D. Burzyn, C. Benoist, D. Mathis. Regulatory T cells in nonlymphoid tissues. Nature immunology; 2013, p. 1007-13.
[41] D. J. Campbell, M. A. Koch. Phenotypical and functional specialization of FOXP3+ regulatory T cells. Nature Reviews Immunology; 2011, p. 119-30.
[42] A. Chaudhry, A. Y. Rudensky. Control of inflammation by integration of environmental cues by regulatory T cells. The Journal of clinical investigation, 2013;123:939-44.
[43] X. Yuan, G. Cheng, T. R. Malek. The importance of regulatory T-cell heterogeneity in maintaining self-tolerance. Immunol Rev; 2014, p. 103-14.
[44] M. Feuerer, L. Herrero, D. Cipolletta, A. Naaz, J. Wong, A. Nayer *et al.* Lean, but not obese, fat is enriched for a unique population of regulatory T cells that affect metabolic parameters. Nat Med, 2009;15:930-9.
[45] E. Sefik, N. Geva-Zatorsky, S. Oh, L. Konnikova, D. Zemmour, A. M. McGuire *et al.* MUCOSAL IMMUNOLOGY. Individual intestinal symbionts induce a distinct population of RORgamma(+) regulatory T cells. Science, 2015;349:993-7.

[46] A. G. Levine, A. Mendoza, S. Hemmers, B. Moltedo, R. E. Niec, M. Schizas *et al.* Stability and function of regulatory T cells expressing the transcription factor T-bet. Nature, 2017;546**:**421-5.
[47] M. M. Barra, D. M. Richards, J. Hansson, A. C. Hofer, M. Delacher, J. Hettinger *et al.* Transcription Factor 7 Limits Regulatory T Cell Generation in the Thymus. J Immunol, 2015;195**:**3058-70.
[48] L. Xu, Q. Huang, H. Wang, Y. Hao, Q. Bai, J. Hu *et al.* The Kinase mTORC1 Promotes the Generation and Suppressive Function of Follicular Regulatory T Cells. Immunity, 2017;47**:**538-51 e5.
[49] M. Miyazaki, K. Miyazaki, S. Chen, M. Itoi, M. Miller, L. F. Lu *et al.* Id2 and Id3 maintain the regulatory T cell pool to suppress inflammatory disease. Nat Immunol, 2014;15**:**767-76.
[50] K. S. Rauch, M. Hils, E. Lupar, S. Minguet, M. Sigvardsson, M. E. Rottenberg *et al.* Id3 Maintains Foxp3 Expression in Regulatory T Cells by Controlling a Transcriptional Network of E47, Spi-B, and SOCS3. Cell Rep, 2016;17**:**2827-36.
[51] W. Lee, H. S. Kim, S. Y. Baek, G. R. Lee. Transcription factor IRF8 controls Th1-like regulatory T-cell function. Cell Mol Immunol, 2016;13**:**785-94.
[52] G. Cheng, X. Yuan, M. S. Tsai, E. R. Podack, A. Yu, T. R. Malek. IL-2 receptor signaling is essential for the development of Klrg1+ terminally differentiated T regulatory cells. J Immunol, 2012;189**:**1780-91.
[53] J. D. Fontenot, M. A. Gavin, A. Y. Rudensky. Foxp3 programs the development and function of CD4+CD25+ regulatory T cells. Nat Immunol, 2003;4**:**330-6.
[54] A. Kallies, J. Hasbold, D. M. Tarlinton, W. Dietrich, L. M. Corcoran, P. D. Hodgkin *et al.* Plasma cell ontogeny defined by quantitative changes in blimp-1 expression. J Exp Med, 2004;200**:**967-77.
[55] Y. Y. Wan, R. A. Flavell. Identifying Foxp3-expressing suppressor T cells with a bicistronic reporter. Proc Natl Acad Sci U S A, 2005;102**:**5126-31.
[56] M. Kamanaka, S. T. Kim, Y. Y. Wan, F. S. Sutterwala, M. Lara-Tejero, J. E. Galan *et al.* Expression of interleukin-10 in intestinal lymphocytes detected by an interleukin-10 reporter knockin tiger mouse. Immunity, 2006;25**:**941-52.
[57] L. Mielke, A. Preaudet, G. Belz, T. Putoczki. Confocal laser endomicroscopy to monitor the colonic mucosa of mice. J Immunol Methods, 2015;421**:**81-8.
[58] H. Mi, S. Poudel, A. Muruganujan, J. T. Casagrande, P. D. Thomas. PANTHER version 10: expanded protein families and functions, and analysis tools. Nucleic Acids Res, 2016;44**:**D336-42.

FIGURE LEGENDS

Figure 1. Blimp-1 is expressed in a subset of mouse T_{reg} and T_{FR} cells. (a) Flow cytometric analysis of splenocytes isolated from an 8-week-old *Foxp3*^{RFP}*Prdm1*^{GFP} reporter mouse. Histogram shows Blimp-1/GFP expression in CD4$^+$Foxp3$^+$ T_{reg} cells (see R1 gate). Data is representative of 5 independent experiments each containing cells isolated from 1-4 mice. **(b)** Percentage of CD4$^+$Foxp3$^+$ T_{reg} cells that are Blimp-1/GFP$^+$ at the sites indicated at 8 weeks and 6 months of age. si (small intestine), IEL (intraepithelial lymphocytes), LPL (lamina propria lymphocytes), mLN (mesenteric lymph nodes), pLN (peripheral lymph nodes) and PP (Peyer's patches). Three *Foxp3*^{RFP}*Prdm1*^{GFP} mice were analyzed by flow cytometry in each group. Data at 8 weeks of age is representative of 2 independent experiments, each containing 3-4 mice. Data are the ± SEM. ** P<0.01, *** P<0.001. **(c)** Flow cytometry analysis of CD4$^+$Foxp3$^+$ T_{reg} cells isolated from the spleen of an 8-week-old *Foxp3*^{RFP}*Prdm1*^{GFP} reporter mouse. Data is representative of 2 independent experiments each containing cells isolated from 3-4 mice. **(d)** PD-1 and CXCR5 expression in CD4$^+$ cells isolated from the mediastinal LN of a *Foxp3*^{RFP}*Prdm1*^{GFP} mouse 9 days after infection with HKx31 influenza virus. Histogram shows Foxp3/RFP expression in CD4$^+$PD-1$^+$CXCR5$^+$ cells (see gate on dot plot). **(e)** Flow cytometry analysis of CD4$^+$PD-1$^+$CXCR5$^+$Foxp3$^+$ T_{FR} cells from **(d)**. Data is representative of 2 independent experiments each containing cells isolated from 3 mice **(d, e)**. Numbers on plots represent the percentage of cells in each quadrant or gate **(a, c, e)**.

Figure 2. Expression of cell surface markers by mouse Blimp-1$^+$ T_{reg} cells. (a) Percentage of Blimp-1/GFP$^+$CD4$^+$Foxp3$^+$ T_{reg} cells that are Nrp-1$^+$, ICOS$^+$ or TIGIT$^+$ at the sites indicated at 8 weeks and 6 months of age. Three *Foxp3*^{RFP}*Prdm1*^{GFP} mice were analyzed by flow cytometry in each group. Data at 8 weeks of age is representative of 2 independent experiments, each containing 3-4 mice. Data are the ± SEM. * P<0.05, ** P<0.01. **(b)** Flow cytometry analysis of CD4$^+$Foxp3$^+$ T_{reg} cells isolated from an 8-week-old *Foxp3*^{RFP}*Prdm1*^{GFP} reporter mouse. SI (small intestine), IEL (intraepithelial lymphocytes), LPL (lamina propria lymphocytes), mLN (mesenteric lymph nodes), pLN (peripheral lymph nodes) and PP (Peyer's patches). Data is representative of 2 independent experiments each containing cells isolated from 3-4 mice. Numbers in quadrants represent the percentage of cells in each**. (c)**

Flow cytometry analysis of $CD4^+Foxp3^+$ T_{reg} cells isolated from the spleen of an 8-week-old *Foxp3*^{RFP}*Prdm1*^{GFP} reporter mouse. Open histogram shows Blimp-1/GFP expression in $CD4^+Foxp3^+$ T_{reg} cells in the R1 ($ICOS^+TIGIT^{+/low}$) gate indicated on the dot plot. Grey closed histogram shows Blimp-1/GFP expression in $CD4^+Foxp3^+$ T_{reg} cells located in the R2 ($ICOS^-TIGIT^-$) gate indicated on the dot plot. Data is representative of 2 independent experiments each containing cells isolated from 3-4 mice. **(d)** Percentage of Blimp-1/GFP^+ and Blimp-1/GFP^- $CD4^+Foxp3^+$ T_{reg} cells within the R1 ($ICOS^+TIGIT^{+/low}$) and R2 ($ICOS^-$ $TIGIT^-$) gates of **(c)** at the tissues indicated. Data show the mean calculated from seven 8-week-old analyzed in 2 independent experiments.

Figure 3. Characterization of Blimp-1-deficient T_{reg} cells. (a) PCR analysis of *Prdm1* gene deletion in *Prdm1*$^{fl/fl}$*Foxp3*$^{YFP\text{-}Cre}$ mice. Genomic DNA was extracted from the tail of a WT (+/+) or *Prdm1*$^{fl/fl}$*Foxp3*$^{YFP\text{-}Cre}$ (fl/fl) mouse, or from FACS-sorted populations of splenocytes isolated from *Prdm1*$^{fl/fl}$*Foxp3*$^{YFP\text{-}Cre}$ or *Foxp3*$^{YFP\text{-}Cre}$ mice as indicated. PCR products represent the WT allele (+, 611 bp), floxed allele (fl, 765 bp) and deletion of the floxed allele (-, 646 bp). The T_{reg} population ($CD4^+Foxp3^+$) was sorted and pooled from the spleens of 3 *Prdm1*$^{fl/fl}$*Foxp3*$^{YFP\text{-}Cre}$ mice. Data is representative of 2 independent experiments, each containing cells sorted from 1-3 mice. **(b)** Flow cytometric analysis of cells isolated from spleen of 8-week-old *Foxp3*$^{YFP\text{-}Cre}$ and *Prdm1*$^{fl/fl}$*Foxp3*$^{YFP\text{-}Cre}$ mice. Shown is the mean fold change of *Prdm1*$^{fl/fl}$*Foxp3*$^{YFP\text{-}Cre}$ mice / *Foxp3*$^{YFP\text{-}Cre}$ mice for the indicated parameter (x axis). **(c)** Flow cytometric analysis of cells isolated from the indicated organ (x axis) of 8-week-old *Foxp3*$^{YFP\text{-}Cre}$ and *Prdm1*$^{fl/fl}$*Foxp3*$^{YFP\text{-}Cre}$ mice. Shown is the mean fold change of *Prdm1*$^{fl/fl}$*Foxp3*$^{YFP\text{-}Cre}$ mice / *Foxp3*$^{YFP\text{-}Cre}$ mice of the proportion of $CD4^+$ T cells that express FoxP3 (left plot) or the proportion of $FoxP3^+$ cells that express ICOS (right plot). Data in **(b-c)** are from 2 independent experiments each containing cells isolated from 3 *Prdm1*$^{fl/fl}$*Foxp3*$^{YFP\text{-}Cre}$ and 1-3 *Foxp3*$^{YFP\text{-}Cre}$ mice. Each dot represents an individual mouse, horizontal lines show the mean ± SEM. * $P<0.05$, ** $P<0.01$, *** $P<0.001$.

Figure 4. Characterization of aged *Prdm1*$^{fl/fl}$*Foxp3*$^{YFP\text{-}Cre}$ mice. (a) Survival graph showing percent survival for 24 *Prdm1*$^{fl/fl}$*Foxp3*$^{YFP\text{-}Cre}$ and 8 wild type C57Bl/6 (WT) mice.

(b) Serum antinuclear antibody concentration in 1 year old WT (n=21) and *Prdm1*$^{fl/fl}$*Foxp3*$^{YFP\text{-}Cre}$ (n=10) mice and in aged *Prdm1*$^{fl/fl}$*Foxp3*$^{YFP\text{-}Cre}$ (n=18) mice at death, relative to the concentration in *Lyn*$^{-/-}$ sera (set to 100). Each dot represents sera from an individual. Horizontal lines show the mean ± SEM. ** P<0.01, *** P<0.001, ns, not significant P>0.05. **(c)** Representative photos of affected organs in four aged *Prdm1*$^{fl/fl}$*Foxp3*$^{YFP\text{-}Cre}$ mice (#168, #294, #170, #185), and from a *Rag1*$^{-/-}$ mouse injected intravenously with $1x10^6$ splenocytes isolated from mouse #168 and harvested when moribund (at 13.6 weeks post-injection). **(d)** Graphs depicting lymphocytic infiltration and tissue damage in the salivary gland, pancreas and gastrointestinal tract of aged mice at death. See Material and Methods for detailed description of the histological scoring. Data are representative of 19 aged *Prdm1*$^{fl/fl}$*Foxp3*$^{YFP\text{-}Cre}$ mice, each harvested the time of culling or death. Each dot represents an individual mouse. Horizontal lines show the mean ± SEM. * P<0.05, *** P<0.001. **(e)** Flow cytometric analysis of $CD4^+Foxp3^+$ T_{reg} cells isolated from an 8-week-old *Foxp3*$^{YFP\text{-}Cre}$ and *Prdm1*$^{fl/fl}$*Foxp3*$^{YFP\text{-}Cre}$ mice and an aged *Prdm1*$^{fl/fl}$*Foxp3*$^{YFP\text{-}Cre}$ mouse at death (69 weeks). Data are representative of 2 independent experiments each containing 1-2 aged *Prdm1*$^{fl/fl}$*Foxp3*$^{YFP\text{-}Cre}$ mice and 1 eight-week-old *Foxp3*$^{YFP\text{-}Cre}$ and *Prdm1*$^{fl/fl}$*Foxp3*$^{YFP\text{-}Cre}$ mouse as well as 1 experiment containing 3 aged *Prdm1*$^{fl/fl}$*Foxp3*$^{YFP\text{-}Cre}$ mice and 1 eight-week-old *Foxp3*$^{YFP\text{-}Cre}$ and *Prdm1*$^{fl/fl}$*Foxp3*$^{YFP\text{-}Cre}$ (spleen and pLN). Numbers show the proportion of cells in each quadrant.

Figure 5. Identification of Blimp-1 regulated genes in T_{reg} cells. Microarray data from [9] showing the comparison of Blimp1/GFP^+ T_{reg} cells from the spleen and lymph nodes of *Prdm1*$^{GFP/+}$ and *Prdm1*$^{GFP/GFP}$ mice. **(a)** Scatter plot of differential expression. Genes with significantly increased (red) or decreased (blue) in the absence of Blimp-1 are indicated (false discovery rate < 0.05). The number of differentially expressed genes is indicated. **(b)** Venn diagram showing overlap and differences between Blimp-1 regulated genes in T_{reg} cells (as in **(a)**) and a published effector T_{reg} cell gene signature [15]. **(c)** Graphs show the fold change (log_2) of the 100 most upregulated (Blimp-1 repressed genes) and downregulated (Blimp-1 activated genes) in the analysis presented in **(a)**. **(d)** Bar chart showing gene ontology classification of differentially expressed genes identified in **(a)** by PANTHER GO-Slim biological process data set (p value <0.05 and fold enrichment > +1). The numbers of

differentially expressed genes in each GO category are indicated. Data in **(a-d)** derive from 3 biologically independent samples for each genotype. **(e)** Quantitative RT-PCR analysis of *Il10* transcripts. $CD4^{+}Foxp3^{+}$ T_{reg} cell populations were sorted from the spleens of $Foxp3^{YFP\text{-}Cre}$, $Foxp3^{RFP}Il10^{GFP}$, $Foxp3^{RFP}Prdm1^{GFP}$ and $Prdm1^{fl/fl}Foxp3^{YFP\text{-}Cre}$ mice. Fold change in *Il10* expression is shown relative to that in $Foxp3^{YFP\text{-}Cre}$ T_{reg} cells (set at 1). Data shown is mean ± SEM from 2 independent experiments with each sample run in triplicate.

Figure 1

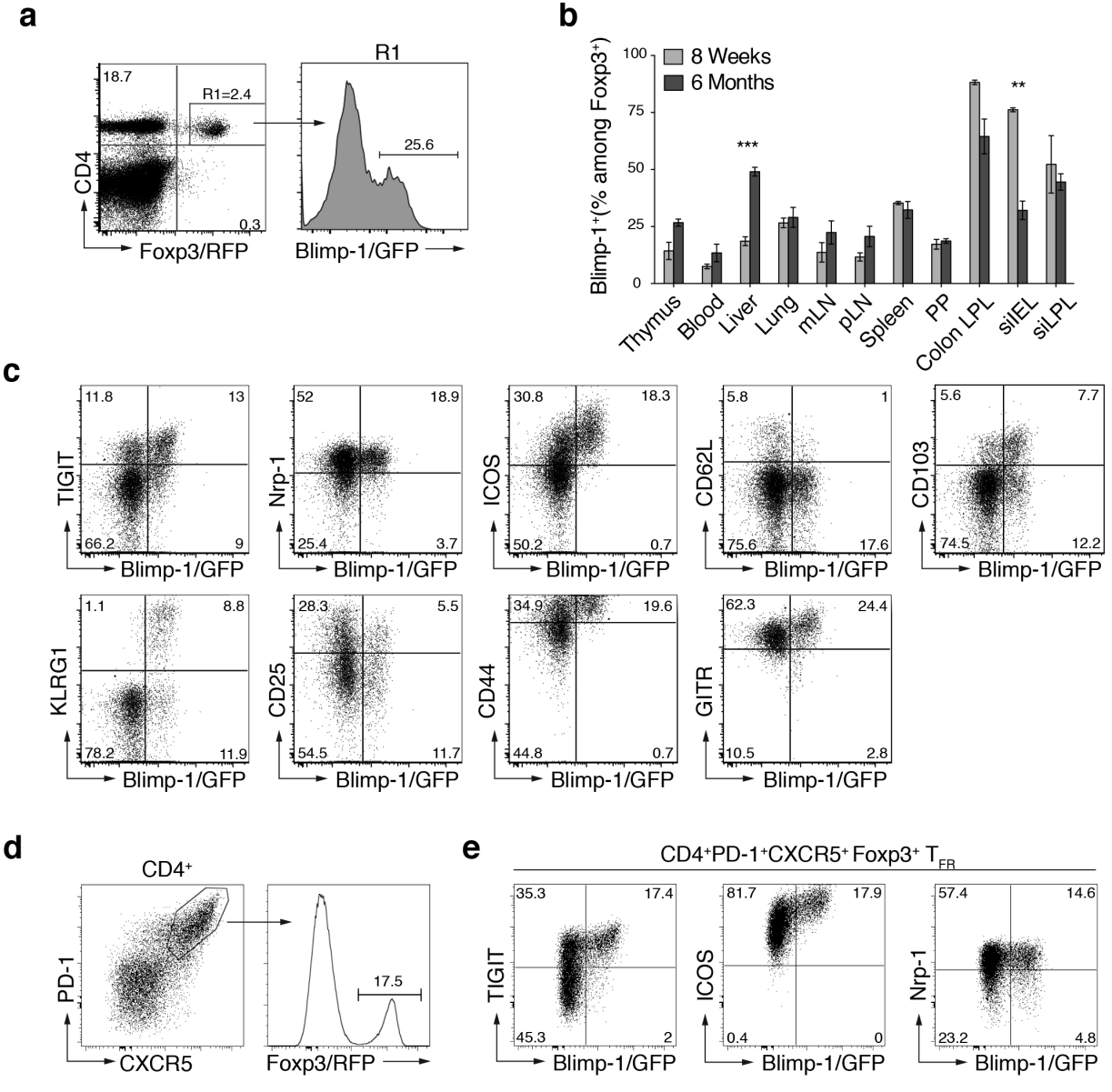
a
R1
18.7
R1=2.4
25.6
0.3
CD4
Foxp3/RFP
Blimp-1/GFP
b
8 Weeks
6 Months
Blimp-1+(% among Foxp3+)
100
75
50
25
0
***
**
Thymus
Blood
Liver
Lung
mLN
pLN
Spleen
PP
Colon LPL
siIEL
siLPL
c
TIGIT
11.8
13
66.2
9
Nrp-1
52
18.9
25.4
3.7
ICOS
30.8
18.3
50.2
0.7
CD62L
5.8
1
75.6
17.6
CD103
5.6
7.7
74.5
12.2
KLRG1
1.1
8.8
78.2
11.9
CD25
28.3
5.5
54.5
11.7
CD44
34.9
19.6
44.8
0.7
GITR
62.3
24.4
10.5
2.8
Blimp-1/GFP
d
CD4+
PD-1
CXCR5
17.5
Foxp3/RFP
e
CD4+PD-1+CXCR5+ Foxp3+ TFR
TIGIT
35.3
17.4
45.3
2
ICOS
81.7
17.9
0.4
0
Nrp-1
57.4
14.6
23.2
4.8
Blimp-1/GFP

Figure 2

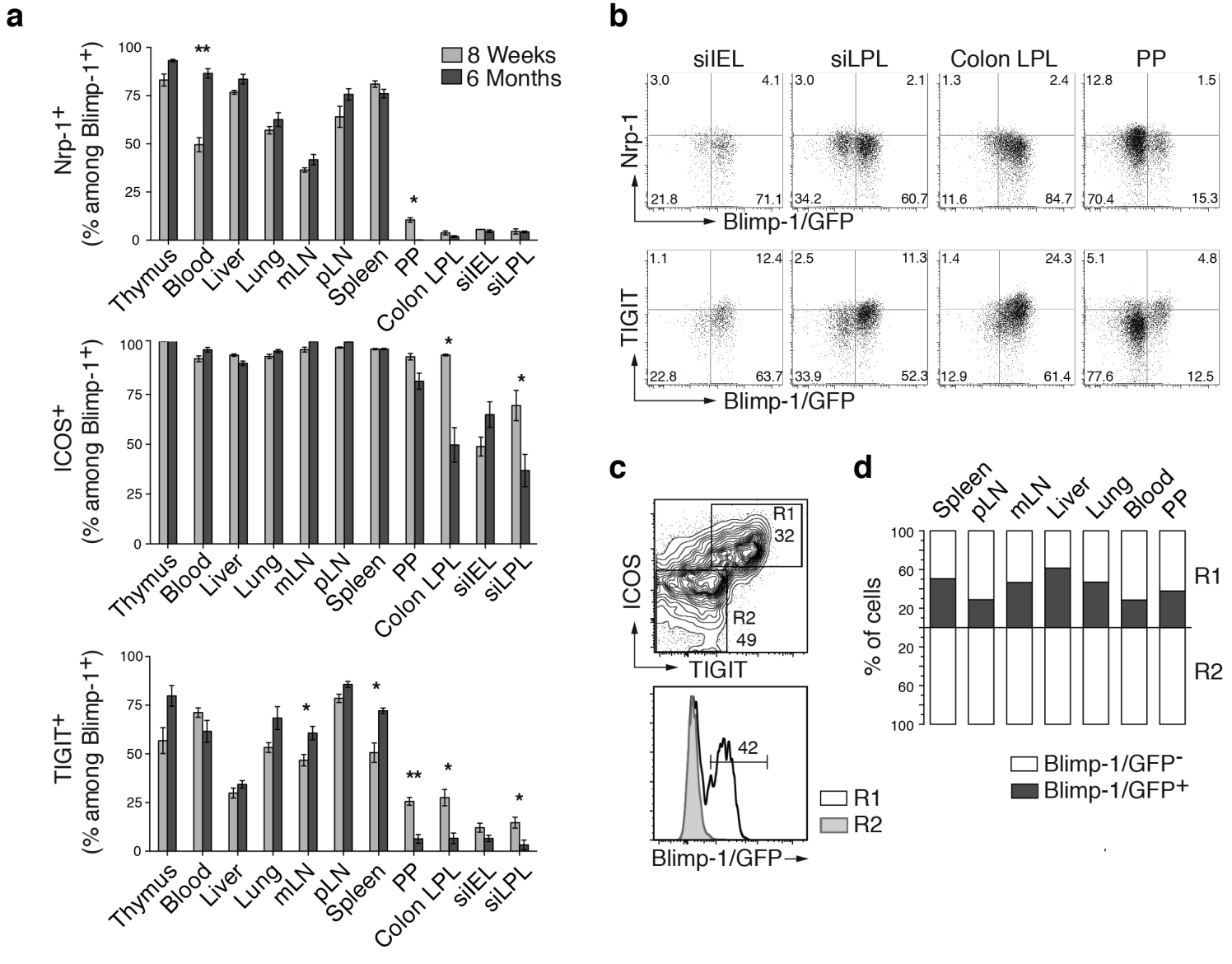
a
8 Weeks
6 Months
Nrp-1+ (% among Blimp-1+)
ICOS+ (% among Blimp-1+)
TIGIT+ (% among Blimp-1+)
Thymus
Blood
Liver
Lung
mLN
pLN
Spleen
PP
Colon LPL
siIEL
siLPL
b
siIEL
siLPL
Colon LPL
PP
Nrp-1
TIGIT
Blimp-1/GFP
c
ICOS
TIGIT
R1
R2
Blimp-1/GFP
d
% of cells
Blimp-1/GFP-
Blimp-1/GFP+

Figure 3

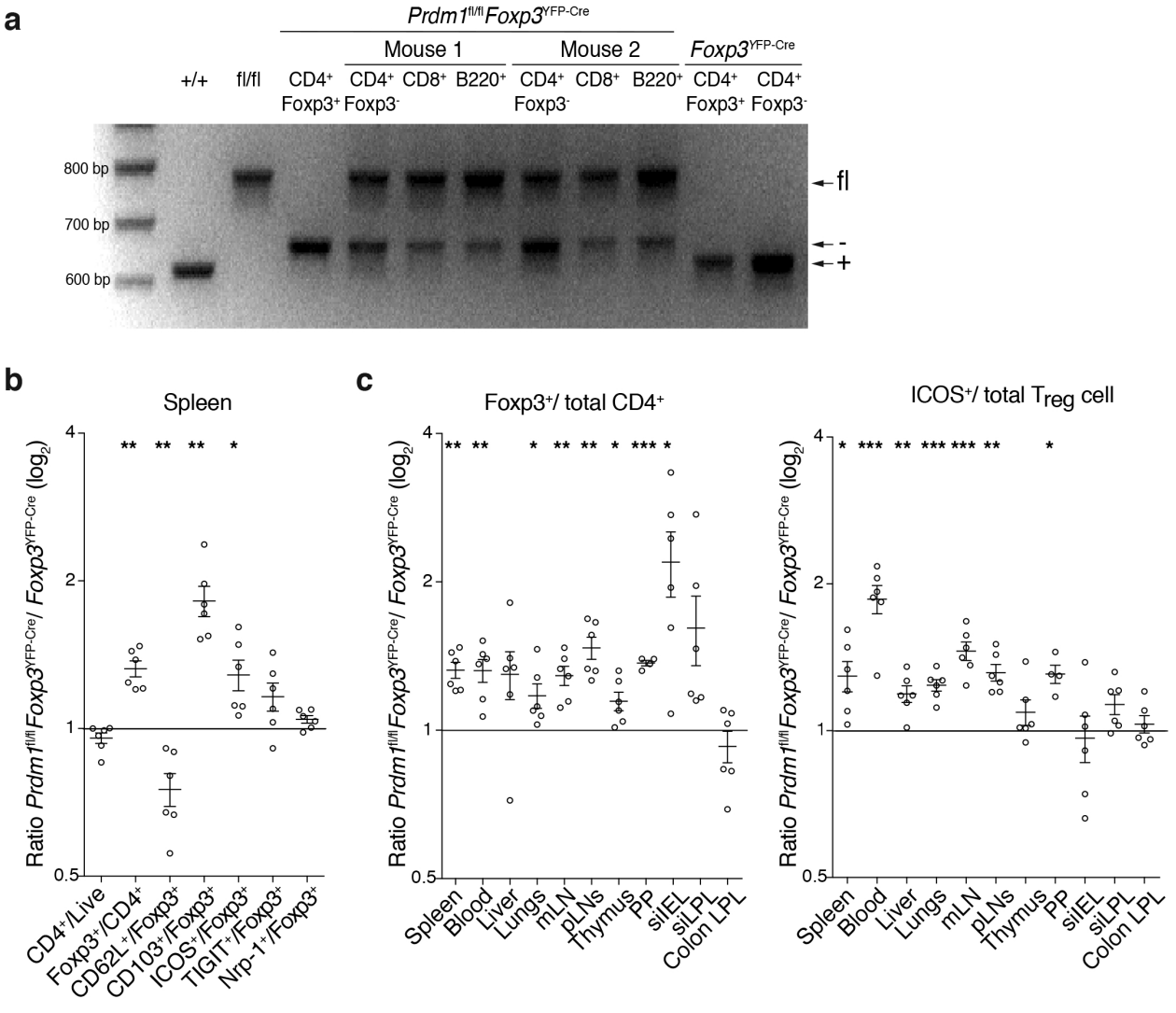
a
Prdm1fl/fl Foxp3YFP-Cre
Mouse 1
Mouse 2
Foxp3YFP-Cre
+/+
fl/fl
CD4+ Foxp3+
CD4+ Foxp3-
CD8+
B220+
CD4+ Foxp3-
CD8+
B220+
CD4+ Foxp3+
CD4+ Foxp3-
800 bp
700 bp
600 bp
fl
-
+
b
Spleen
Ratio Prdm1fl/fl Foxp3YFP-Cre/ Foxp3YFP-Cre (log2)
CD4+/Live
Foxp3+/CD4+
CD62L+/Foxp3+
CD103+/Foxp3+
ICOS+/Foxp3+
TIGIT+/Foxp3+
Nrp-1+/Foxp3+
c
Foxp3+/ total CD4+
ICOS+/ total Treg cell
Spleen
Blood
Liver
Lungs
mLN
pLNs
Thymus
PP
siIEL
siLPL
Colon LPL

Figure 4

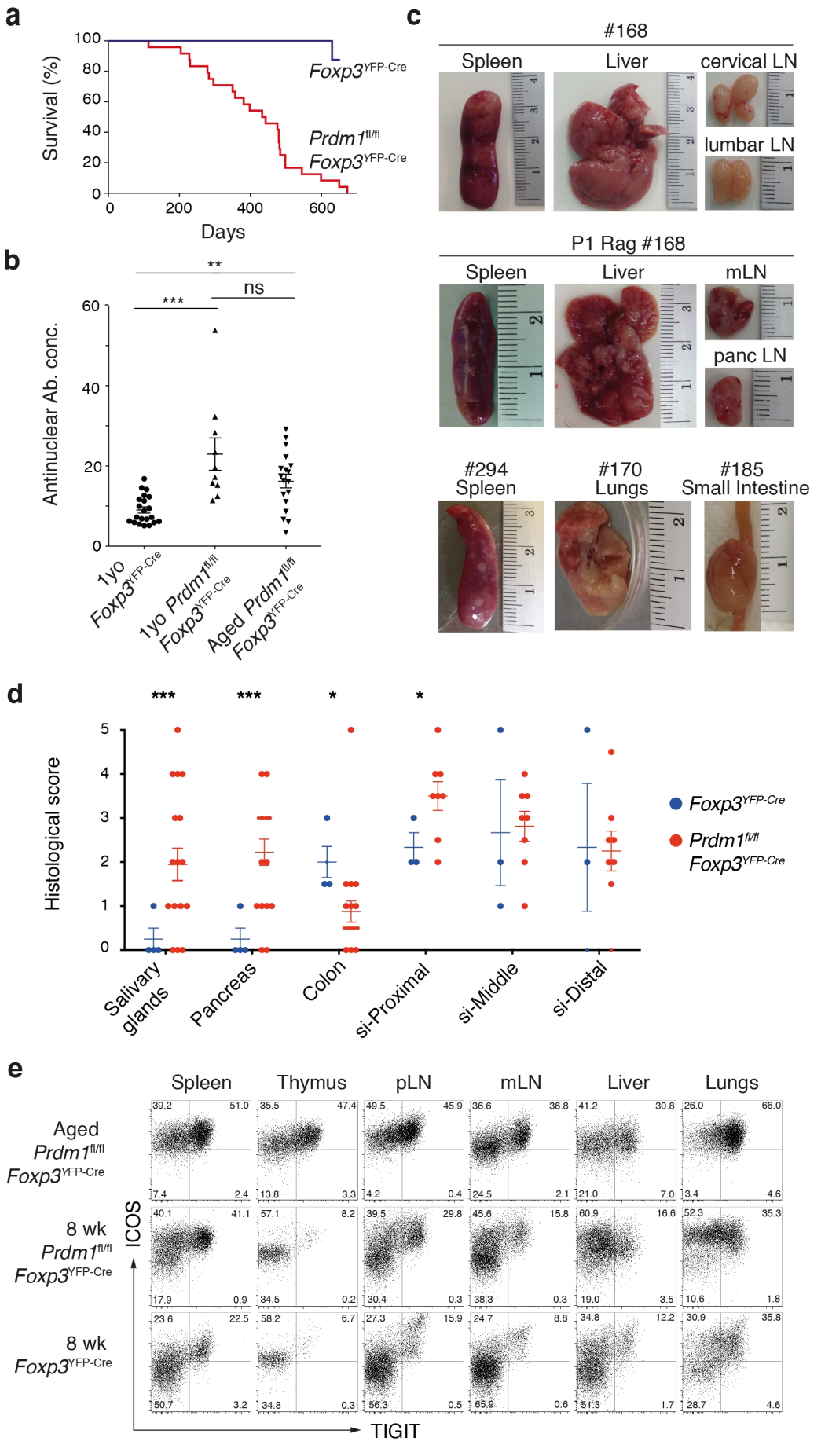
a
Survival (%)
Days
Foxp3YFP-Cre
Prdm1fl/fl Foxp3YFP-Cre
b
Antinuclear Ab. conc.
**
***
ns
1yo Foxp3YFP-Cre
1yo Prdm1fl/fl Foxp3YFP-Cre
Aged Prdm1fl/fl Foxp3YFP-Cre
c
#168
Spleen
Liver
cervical LN
lumbar LN
P1 Rag #168
Spleen
Liver
mLN
panc LN
#294 Spleen
#170 Lungs
#185 Small Intestine
d
Histological score
Salivary glands
Pancreas
Colon
si-Proximal
si-Middle
si-Distal
Foxp3YFP-Cre
Prdm1fl/fl Foxp3YFP-Cre
e
Spleen
Thymus
pLN
mLN
Liver
Lungs
Aged Prdm1fl/fl Foxp3YFP-Cre
8 wk Prdm1fl/fl Foxp3YFP-Cre
8 wk Foxp3YFP-Cre
ICOS
TIGIT

figure 5

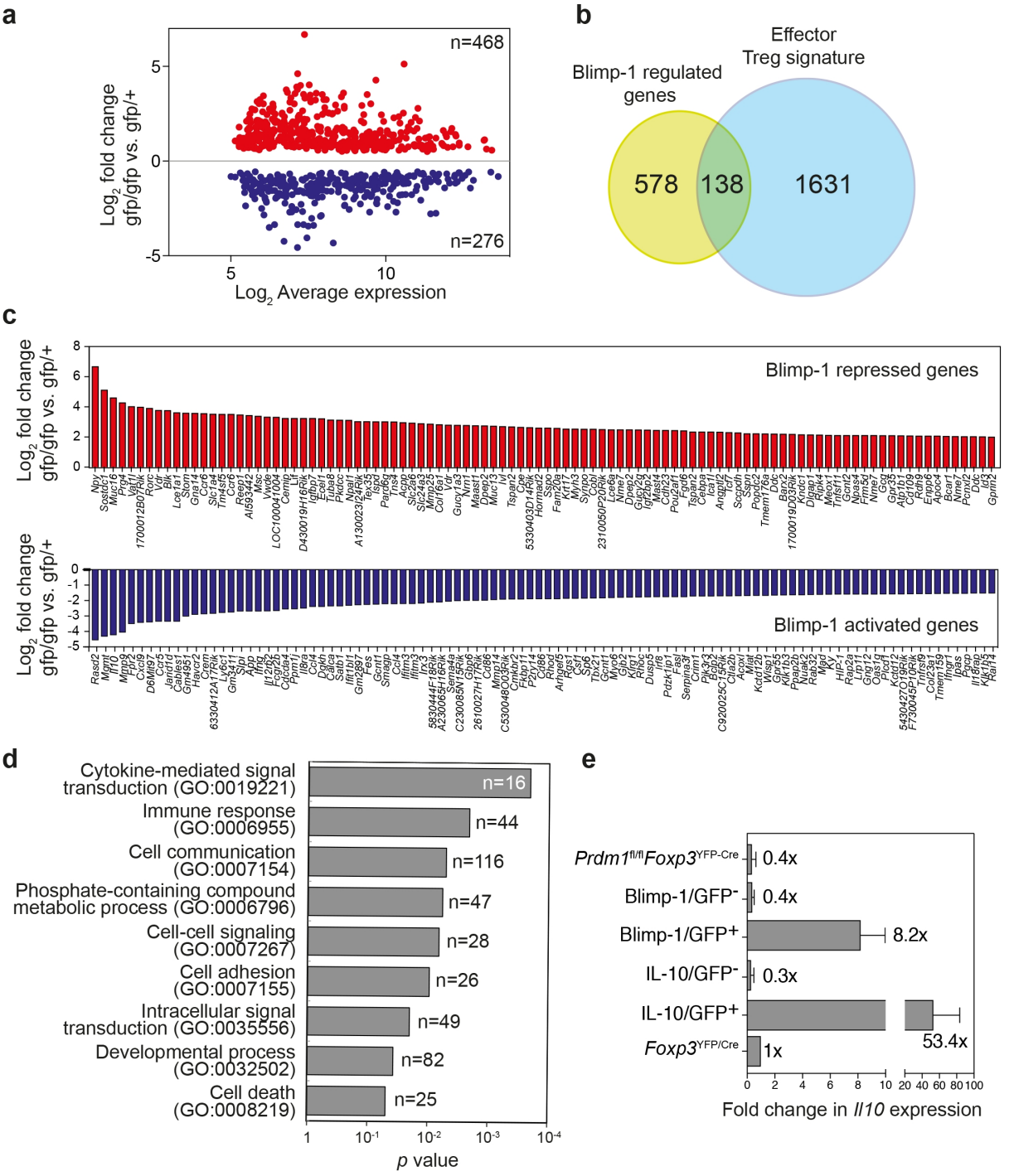
a
n=468
n=276
Log2 fold change gfp/gfp vs. gfp/+
Log2 Average expression
b
Blimp-1 regulated genes
Effector Treg signature
578
138
1631
c
Blimp-1 repressed genes
Blimp-1 activated genes
Log2 fold change gfp/gfp vs. gfp/+
d
Cytokine-mediated signal transduction (GO:0019221)
Immune response (GO:0006955)
Cell communication (GO:0007154)
Phosphate-containing compound metabolic process (GO:0006796)
Cell-cell signaling (GO:0007267)
Cell adhesion (GO:0007155)
Intracellular signal transduction (GO:0035556)
Developmental process (GO:0032502)
Cell death (GO:0008219)
n=16
n=44
n=116
n=47
n=28
n=26
n=49
n=82
n=25
p value
e
Prdm1fl/flFoxp3YFP-Cre
Blimp-1/GFP-
Blimp-1/GFP+
IL-10/GFP-
IL-10/GFP+
Foxp3YFP/Cre
0.4x
0.4x
8.2x
0.3x
53.4x
1x
Fold change in Il10 expression

SUPPLEMENTARY MATERIAL

Characterization of Blimp-1 function in effector regulatory T cells

Erika Cretney[1,2], Patrick SK Leung[1,2], Stephanie Trezise[1,2], Dane M Newman[1,2], Lucille C Rankin[1,2], Charis E Teh[1,2], Tracy L Putoczki[1,2], Daniel H D Gray[1,2], Gabrielle T Belz[1,2], Lisa A Mielke[1,2], Sheila Dias[1,2], Stephen L Nutt[1,2].

[1]The Walter and Eliza Hall Institute of Medical Research, Parkville, Victoria, Australia.
[2]Department of Medical Biology, The University of Melbourne, Parkville, Victoria, Australia.

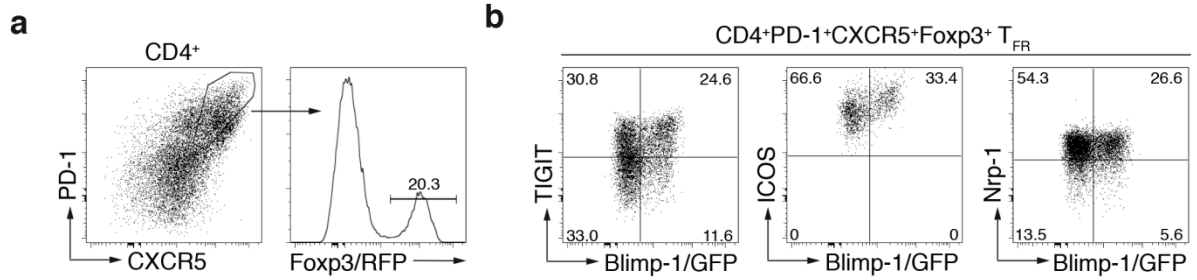

Supplementary Figure 1. Blimp-1 is expressed in splenic T follicular regulatory cells following influenza infection. (a) PD-1 and CXCR5 expression in $CD4^+$ cells isolated from the spleen of a *Foxp3*^{RFP}*Prdm1*^{GFP} mouse 9 days after infection with HKx31 influenza virus. Histogram shows Foxp3/RFP expression in $CD4^+PD\text{-}1^+CXCR5^+$ cells (see gate). **(b)** Flow cytometry analysis of $CD4^+PD\text{-}1^+CXCR5^+Foxp3^+$ T_{FR} cells isolated as in **(a)**. Data is representative of 2 independent experiments each containing cells isolated from 3 *Foxp3*^{RFP}*Prdm1*^{GFP} mice. Numbers indicate the proportion of cells in each gate or quadrant.

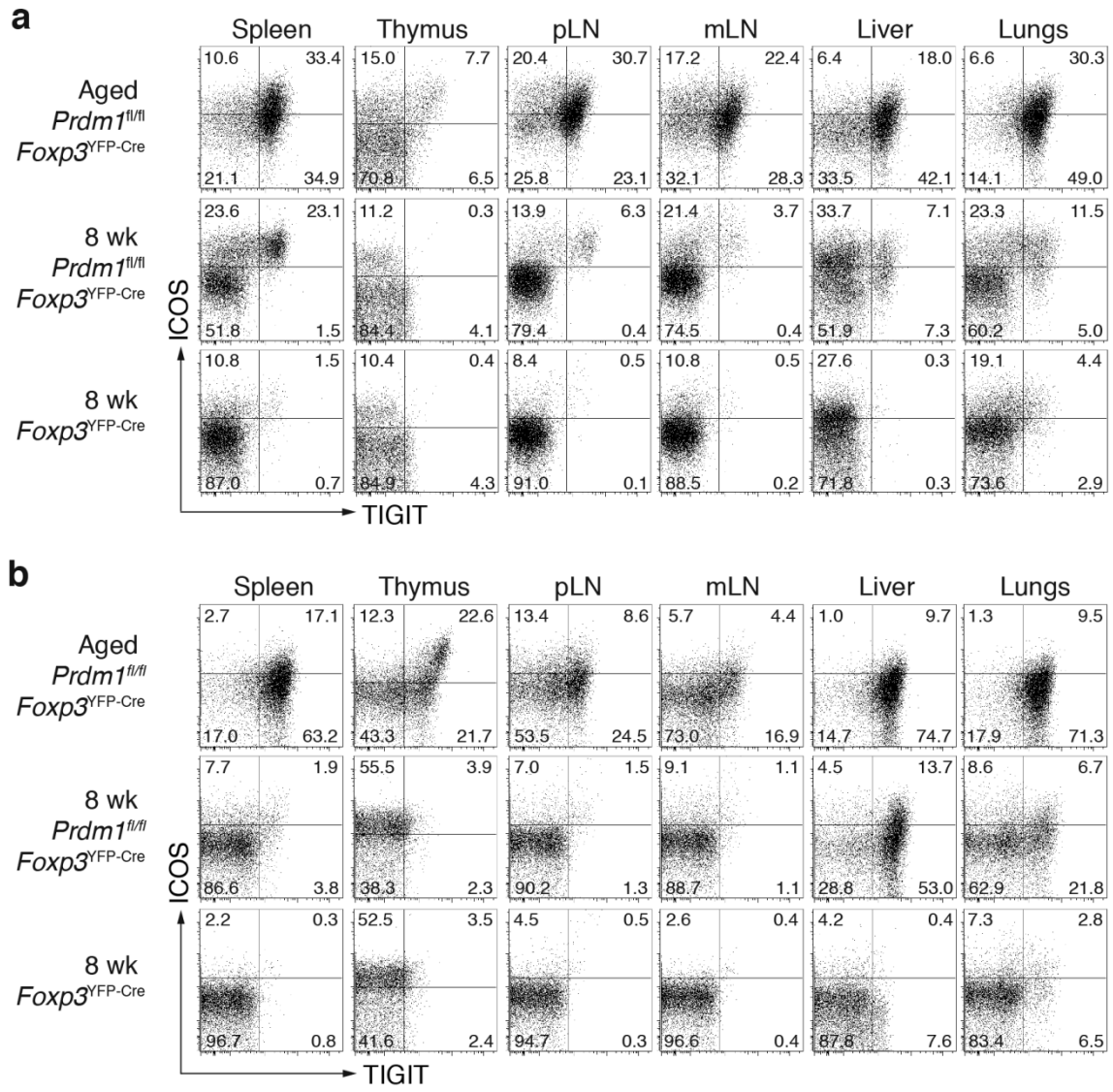

Supplementary Figure 2. Increased ICOS and TIGIT expression in CD4$^+$Foxp3$^-$ and CD8$^+$ cells isolated from aged *Prdm1*$^{fl/fl}$*Foxp3*$^{YFP\text{-}Cre}$ mice. (a) Flow cytometric analysis of CD4$^+$Foxp3$^-$ and **(b)** CD8$^+$ cells isolated from 8 week old *Foxp3*$^{YFP\text{-}Cre}$ and *Prdm1*$^{fl/fl}$*Foxp3*$^{YFP\text{-}Cre}$ mice and an aged *Prdm1*$^{fl/fl}$*Foxp3*$^{YFP\text{-}Cre}$ mouse at death (69 weeks). Data are representative of 3 independent experiments each containing 1-3 aged *Prdm1*$^{fl/fl}$*Foxp3*$^{YFP\text{-}Cre}$ mice and 1 eight week old *Foxp3*$^{YFP\text{-}Cre}$ and *Prdm1*$^{fl/fl}$*Foxp3*$^{YFP\text{-}Cre}$ mouse (spleen and pLN) and 2 independent experiments containing 1-2 aged *Prdm1*$^{fl/fl}$*Foxp3*$^{YFP\text{-}Cre}$ mice and 1 eight week old *Foxp3*$^{YFP\text{-}Cre}$ and *Prdm1*$^{fl/fl}$*Foxp3*$^{YFP\text{-}Cre}$ mouse (thymus, mLN, liver, lung). Numbers indicate the proportion of cells in each quadrant.

Supplementary Table 1. Flow cytometry antibodies and detection agents

Target/ Detection	Fluorophore/ Conjugate	Clone	Supplier
Anti-Rat	Biotin		Life Technologies
Anti-Rat	Cy5		Life Technologies
B220	PE	RA3-6B2	eBioscience
CD103	Biotin	M290	BD
CD103	PCPeF710	2E7	eBioscience
CD25	PCPCy5.5	PC61.5	eBioscience
CD25	PECy7	PC61.5	eBioscience
CD25	PE	PC61	eBioscience
CD4	AF680	GK1.5	Produced in house
CD4	FITC	GK1.5	Produced in house
CD4	PB	GK1.5	Produced in house
CD4	PECy7	GK1.5	Biolegend
CD44	PECy7	IM7	eBioscience
CD8α	A680	53.6.7	Produced in house
CD8α	APC	53.6.7	Produced in house
CD8α	PE	YTS169	Produced in house
CD62L	APC	MEL-14	BD
CXCR5	Purified	2G8	BD
FoxP3	PB	FJK-16s	eBioscience
FoxP3	PCPCy5.5	FJK-16s	eBioscience
FoxP3	PE	FJK-16s	eBioscience
GITR	APC	DTA-1	eBioscience
ICOS (CD278)	PE	7E.17G9	eBioscience
ICOS (CD278)	PECy7	7E.17G9	eBioscience

ICOS (CD278)	PCPCy5.5	15F9	Biolegend
KLRG1	APC	2F1	eBioscience
Neuropilin-1	APC	761705	R&D
PD-1 (CD279)	PECy7	RMPI-30	Biolegend
Streptavidin	Brilliant Violet 570		Biolegend
Streptavidin	PCPCy5.5		eBioscience
Streptavidin	PECy7		Biolegend
TCRβ	APC	H57-597	BD
TIGIT	eF660	GIGD7	eBioscience
TIGIT	PCPeF710	GIGD7	eBioscience